

# Characterization of 25 Tropical Hardwoods with Fourier Transform Infrared, Ultraviolet Resonance Raman, and $^{13}\text{C}$ -NMR Cross-Polarization/Magic-Angle Spinning Spectroscopy

Mari H. Nuopponen,<sup>1</sup> Hanne I. Wikberg,<sup>2</sup> Gillian M. Birch,<sup>1</sup> Anna-Stiina Jääskeläinen,<sup>3</sup> Sirkka L. Maunu,<sup>2</sup> Tapani Vuorinen,<sup>3</sup> Derek Stewart<sup>1</sup>

<sup>1</sup>Scottish Crop Research Institute, Invergowrie, Dundee DD2 5DA, Scotland, United Kingdom

<sup>2</sup>Laboratory of Polymer Chemistry, University of Helsinki, P.O. Box 55, FIN-00014 University of Helsinki, Finland

<sup>3</sup>Laboratory of Forest Products Chemistry, Helsinki University of Technology, P.O. Box 6300, FIN-02015 TKK, Finland

Received 7 July 2005; accepted 9 January 2006

DOI 10.1002/app.24143

Published online in Wiley InterScience (www.interscience.wiley.com).

**ABSTRACT:** Twenty-five tropical hardwoods from Ghana were examined with Fourier transform infrared (FTIR), ultraviolet resonance Raman (UVRR), and  $^{13}\text{C}$ -NMR cross-polarization/magic-angle spinning spectroscopy. FTIR and UVRR spectral data were subjected to principal component analysis, whereas four selected samples exhibiting large structural and compositional variation were investigated in more detail by NMR spectroscopy. The acetyl bromide lignin and  $\alpha$ -cellulose contents of the samples and the amount of acetone-soluble substances were also determined. The most prominent principal components of the FTIR spectral model separated samples mainly due to the variations in lignin structures and carbohydrate contents and the amount and type of carbonyl structures, whereas UVRR spectral data distinguished between various aromatic and other un-

saturated structures. The presence of condensed lignin/tannin-type structures were detected from UVRR and FTIR loading line plots of the minor principal components. Condensed tannins were also observed in the dipolar dephasing NMR spectra. Furthermore, the NMR results showed variations in the amount of crystalline cellulose and hemicelluloses and in the syringyl/guaiacyl proportions in lignin. Both NMR and FTIR data suggest that in most cases, a higher amount of guaiacyl units correlated with higher levels of acetyl bromide lignin and better bioresistance of the samples. © 2006 Wiley Periodicals, Inc. *J Appl Polym Sci* 102: 810–819, 2006

**Key words:** FTIR; NMR; Raman spectroscopy

## INTRODUCTION

Some tropical woods, such as teak (*Tectona grandis* L.f.), are known to have good natural durability against decay, insect attack, and weathering and have been used in many outdoor applications including boats, decking, and outdoor furniture.<sup>1</sup> Consequently, the fungal durability<sup>2,3</sup> and weathering resistance<sup>4,5</sup> of tropical hardwoods has been of continued interest to researchers. The fungal durability of tropical hardwoods has been associated with certain extractable compounds,<sup>6</sup> for example, the biological resistances of iroko and opepe have been related to chlorophorin and indole-pyridin alkaloids, respectively.<sup>3</sup> The demand for high-quality wood is increasing in global markets, and thus, a better knowledge of the properties of lesser known tropical woods is of great economic importance.

The chemical composition of tropical hardwoods differs from temperate-zone hardwoods. The lignin content of tropical hardwoods can exceed that of softwoods and has been reported to be in the range of 29.4–40.5% (w/w).<sup>7–10</sup> Fengel et al.<sup>8</sup> found that the amount of syringyl (S) lignin is lower for some tropical hardwoods (*Lophira alata*, *Ochroma lagopus*, and *Araucaria angustifolia*) than for temperate-zone hardwoods. Furthermore, they reported that the structure of lignin in tropical hardwoods was more oxidized.

Fourier transform infrared (FTIR) spectroscopy has been used to characterize the molecular structures of various tropical hardwoods.<sup>4,8,11,12</sup>  $^{13}\text{C}$ -NMR cross-polarization/magic-angle spinning (CP-MAS) spectroscopy has been successfully applied in numerous studies of temperate-zone softwoods and hardwoods and their components, whereas tropical woods have been studied less extensively.<sup>12–15</sup> Ultraviolet resonance Raman (UVRR) spectroscopy is a relatively recent technique in the field of wood chemistry, and its applications include studies of lignin model compounds<sup>16</sup> and chemical changes in heat-treated wood,<sup>17</sup> the determination of lignin and hexenuronic

Correspondence to: M. H. Nuopponen (mnuopponen@herc.com).

TABLE I  
Tropical Hardwood Samples from Ghana

Sample number and common name	Scientific name	Family
19. Aprozuma	<i>Antrocaryon micraster</i>	Anacardiaceae
1. Idigbo	<i>Terminalia ivorensis</i>	Combretaceae
17. Afara	<i>Terminalia superba</i>	Combretaceae
5. Kokrodua	<i>Pericopsis elata</i>	Leguminosae
6. Cobaiba	<i>Copaifera spp.</i>	Leguminosae
7. Dahoma	<i>Piptadeniastrum africanum</i>	Leguminosae
8. Ogea	<i>Daniellia ogea</i>	Leguminosae
15. Awiemfo samina	<i>Albizzia ferruginea</i>	Leguminosae
4. African mahogany	<i>Khaya ivorensis</i>	Meliaceae
12. Avodire	<i>Turreanthus africanus</i>	Meliaceae
13. Sapele	<i>Entandrophragma cylindricum</i>	Meliaceae
14. Scented guarea	<i>Guarea cedrata</i>	Meliaceae
16. Kosipo	<i>Entandrophragma candollei</i>	Meliaceae
22. Cedro	<i>Cedrela mexicana</i>	Meliaceae
25. African walnut	<i>Lovoa trichilioides</i>	Meliaceae
3. Iroko	<i>Chlorophora excelsa</i>	Moraceae
10. Ekki	<i>Lophira alata</i>	Ochnaceae
9. Kokoti	<i>Anopyxis klaineana sprague</i>	Rhizophoraceae
2. Abura	<i>Mitragyna ciliata</i>	Rubiaceae
21. Opepe	<i>Nauclea diderichii</i>	Rubiaceae
20. Makore	<i>Tieghemella heckelii</i>	Sapotaceae
11. Mansonia	<i>Mansonia altissima</i>	Sterculiaceae
23. Nyankom	<i>Tarrietia utilis</i>	Sterculiaceae
24. Obeche	<i>Triplochiton scleroxylon</i>	Sterculiaceae
18. Danta	<i>Nesogordonia papaverifera</i>	Sterculiaceae

acid contents in bleached chemical pulps,<sup>18</sup> and the identification of extractable compounds in wood.<sup>19,20</sup> The resonance Raman effect occurs if the excitation wavelength lies close to an electronic absorption of a particular structure within a molecule. Thus, the signals from such structures can be enhanced by several orders of magnitude. UV excitation causes the enhancement of band intensities attributed to aromatic and other unsaturated structures in wood, and therefore, spectra containing signals derived only from lignin and other unsaturated structures can be obtained. The objective of this study was to apply different spectroscopic techniques in the solid state, FTIR, UVRR, and <sup>13</sup>C-NMR CP-MAS, to explore the chemical structure and, therefore, phytochemical diversity of different tropical hardwoods from Ghana. The advantage of these techniques is that the samples can be studied in the solid state, so minimal preparation is required. Acetone-extracted samples were analyzed with FTIR and UVRR, and unextracted samples were measured with NMR. Moreover, the lignin and  $\alpha$ -cellulose contents of the samples were determined gravimetrically.

## EXPERIMENTAL

### Sample preparation

The tropical hardwood samples from Ghana (a gift from B. Gardiner, Forest Research, Edinburgh, UK)

are listed in Table I. Samples for the FTIR and UVRR measurements were ground in a Glen Creston laboratory mill to pass a 500- $\mu$ m sieve. Wood extractives were removed from the ground wood samples (0.5 g) by Soxhlet extraction for 3 h with acetone. Extracts were evaporated to dryness by rotary evaporation and were then weighed. Unextracted samples were measured with NMR.

### $\alpha$ -Cellulose

$\alpha$ -Cellulose was isolated from duplicate samples (50 mg of the extractive free sample) according to a method of Brendel et al.<sup>21</sup>

### Lignin

The lignin contents of the extractive free samples (5 mg) were determined in triplicate with the acetyl bromide method.<sup>22</sup> In this method, lignocellulosic samples are dissolved in a mixture of acetyl bromide and glacial acetic acid (1 : 3 v/v), and the absorbance at 280 nm is measured. The acetyl bromide method is often used to determine lignin content when the sample amount is too low for the Klason method. It is known that the acetyl bromide method gives a somewhat lower lignin content than the Klason method.<sup>23</sup>

## FTIR

FTIR spectra of the ground wood samples were acquired with a Bruker IFS 66 spectrometer (Bruker Optics Inc., Ettlingen, Germany) with a Specac DRIFT accessory over the range 4000–400  $\text{cm}^{-1}$  and with a resolution of 4  $\text{cm}^{-1}$ . A deuterated triglycine sulfate (DTGS) detector was used. Four hundred scans were accumulated before the Fourier transformation. IR spectra were expressed in the values of the Kubelka–Munk function.

## UVR

Acetone-extracted and ground wood samples (20 mg) were mixed with KBr (200 mg) and pressed into pellets before the UVR analysis. UVR spectra were collected with a Renishaw 1000 UV Raman spectrometer (Gloucestershire, UK) coupled to an Innova 90C FreD frequency-doubled Ar<sup>+</sup> ion laser (Coherent, Inc., Santa Clara, CA) tuned to a wavelength of 244 nm. The spectra were collected at 1.3 mW of power at the sample level; the total spectral collection time was  $60 \times 10$  s. The spectra were collected through a Leica DMLM microscope (Leica Microsystems GmbH, Wetzlar, Germany) (15 $\times$  objective), and a UV-coated charged coupling device camera was used for detection. The samples were spun during the measurement to avoid the burning of the sample. The spectral range was 400–2400  $\text{cm}^{-1}$ , and the resolution was about 7  $\text{cm}^{-1}$ .

## <sup>13</sup>C-NMR CP–MAS spectroscopy

<sup>13</sup>C-NMR CP–MAS spectra were acquired on a Varian Unity Inova 300-MHz spectrometer (Varian Assoc., Palo Alto, CA) operating at 75.47 Hz for carbon. For all of the wood samples, the spinning speed was 5000 Hz, the contact time was 1 ms, the acquisition time was 20 ms, and the delay between pulses was 2 s. Samples were moistened with deionized water for 1 h before the measurements because hydration is well-reported to improve the signal-to-noise ratio.<sup>24,25</sup>

The dipolar dephasing (DD) technique is a useful technique for studying lignin in wood because it suppresses the signals from protonated carbons, so that the quaternary carbons of lignin can be studied in more detail.<sup>26–29</sup> In DD measurements, the high-power decoupler is turned off for 50  $\mu\text{s}$  before data acquisition. The chemical shifts in the spectra were referenced to the cellulose C-1 signal at 105 ppm in the CP–MAS spectra and to the methoxyl signal at 56 ppm in the DD spectra.

## Principal component analysis (PCA)

PCA for the untreated spectral data was performed with a Simca-P 10.1 software package (Umetrics Inc.,

Umeå, Sweden). IR spectral data was mean-centered before analysis. UVR data was pretreated with the standard normal variate procedure and centered before the calculation of the principal components. Only the first four principal components were used for the characterization of the spectral data. The most prominent component of the UVR and FTIR models was the first one, which accounted for 56 and 87% of the variation, respectively, whereas the other components explained only 2–6% of the variation between the wood samples. However, the loading line plots of the minor components revealed noticeable spectral differences due to the various chemical structures, and the results were in line with the comparisons made directly from the spectra.

## RESULTS

The  $\alpha$ -cellulose and acetyl bromide lignin contents and the amounts of acetone-soluble substances of the tropical hardwoods are listed in Table II. The  $\alpha$ -cellulose contents of the samples were in the range 42–48% (w/w), and the acetyl bromide lignin contents varied between 19 and 31% (w/w).

## FTIR spectroscopy

PCA was performed to identify the IR spectral characteristics of the tropical hardwoods. The first principal components of the PCA model originated from intensity variations; the second one was not informative, and therefore, they are not presented here. In addition to the PCA of the IR spectral data, four selected FTIR spectra were characterized separately in more detail. The third and fourth principal components segregated the samples into groups (Fig. 1). Loading line plots revealed spectral differences beyond the clustering of the samples (Figs. 2 and 3). Both loadings exhibited strong bands at 1740 and 1244  $\text{cm}^{-1}$ , which were assigned to C=O and C–O vibrations of the acetyl groups in hardwood xylans (Figs. 2 and 3).<sup>30</sup> The third loadings (Fig. 2) also showed a fairly strong positive band at 1134  $\text{cm}^{-1}$ , which most likely originated from the glycosidic C–O–C vibration of xylan.<sup>31</sup> The other bands at 1589, 1500, 1462, 1424, 1330, and 827  $\text{cm}^{-1}$  in Figure 2 were consistent with those in the spectrum of S lignin.<sup>32</sup> This indicates that the samples with positive scores in the direction of the third principal component may have contained more S units, especially samples 18 and 19, than the samples located on the negative side.

In addition, positive bands in the loadings of the fourth principal component (Fig. 3) showed bands at 1668, 1650–1600, 1513, and 1068  $\text{cm}^{-1}$ . The absorption at 1668  $\text{cm}^{-1}$  was assigned to conjugated carbonyl structures, whereas the signals in the wave-number region of 1650–1600 could have included vibrations

TABLE II  
Acetyl Bromide Lignin and  $\alpha$ -Cellulose Contents, Densities, and Durability Classes  
of Tropical Hardwood Samples from Ghana

Sample number and common name	Acetyl bromide lignin (wt %)	$\alpha$ -Cellulose (wt %)	Extractable compounds (wt %) <sup>a</sup>	Durability class	Density (kg/m <sup>3</sup> )
1. Idigbo	28.4	42.2	6.6	Durable <sup>b</sup>	383
2. Abura	26.7	38.1	1.8	Low <sup>b</sup>	529
3. Iroko	26.7	36.6	5.3	Very durable <sup>b</sup>	514
4. African mahogany	23.7	37.9	1.4	Moderate <sup>b</sup>	468
5. Kokrodua	31.1	36.6	4.3	Very durable <sup>b</sup>	744
6. Cobaiba	26.7	41.8	2.4	Low <sup>c</sup>	791
7. Dahoma	24.4	41.4	0.9	Moderate <sup>b</sup>	615
8. Ogea	19.9	46.9	1.3	Low <sup>b</sup>	532
9. Kokoti	24.1	41.9	1.1	Low <sup>b</sup>	878
10. Ekki	23.6	47.8	0.6	Durable <sup>b</sup>	1121
11. Mansonia	26.1	38.5	4.2	Very durable <sup>b</sup>	644
12. Avodire	23.9	42.4	3.3	Low <sup>b</sup>	550
13. Sapele	23.3	35.2	1.5	Moderate <sup>b</sup>	689
14. Scented guarea	25.7	37.2	3.1	Moderate <sup>b</sup>	623
15. Awiemfo samina	27.8	40.1	4.3	Moderate <sup>b</sup>	591
16. Kosipo	24.2	35.4	0.5	Moderate <sup>b</sup>	591
17. Afara	26.3	40.8	1.4	Low <sup>b</sup>	474
18. Danta	26.3	32.0	2.4	Moderate <sup>b</sup>	747
19. Aprozuma	19.3	47.0	0.6	Low <sup>b</sup>	441
20. Makore	24.6	35.4	3.6	Very durable <sup>b</sup>	606
21. Opepe	31.0	43.1	1.6	Very durable <sup>b</sup>	705
22. Cedro	25.2	39.6	2.8	Durable <sup>c</sup>	353
23. Nyankom	26.3	39.2	3.5	Moderate <sup>b</sup>	602
24. Obeche	28.5	38.5	1.3	Low <sup>b</sup>	398
25. African walnut	26.8	40.4	2.1	Moderate <sup>b</sup>	621

<sup>a</sup> Amount of compounds soluble in acetone (wt %).

<sup>b</sup> Data from <http://www2.fpl.fs.fed.us/TechSheets/tropicalwood.html>.

<sup>c</sup> Data from <http://www.cirad.fr/activites/bois/en/syst/america>.

from conjugated/aromatic carbonyl groups and aromatic rings. The band at  $1513\text{ cm}^{-1}$  was associated with asymmetric aromatic ring stretch.<sup>33</sup> Previously, the band at  $1620\text{ cm}^{-1}$  in the FTIR spectra of the hardwood milled wood lignin lignins has been assigned to tannins.<sup>12</sup> Soluble tannins can be extracted

from wood with various polar solvents, such as acetone, methanol, and ethanol. In addition to soluble tannins, the occurrence of insoluble condensed tannins is well known, and they have been reported to associate with cell-wall polymers.<sup>34,35</sup> Thus, the bands in the loading line plot indicated that the samples with

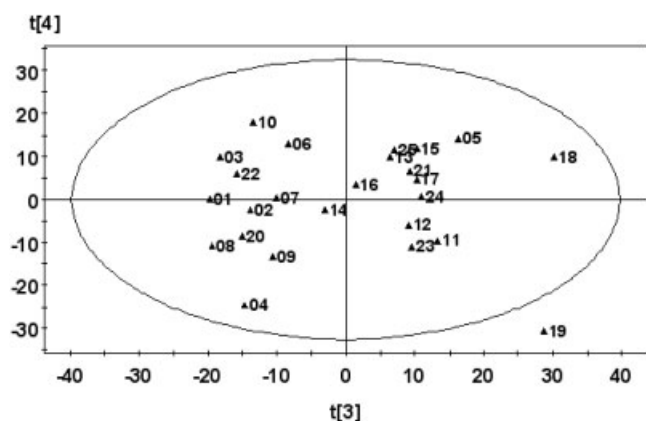


Figure 1 Score scatter plot of the third and fourth principal components of the FTIR spectral data of the extracted hardwood samples.

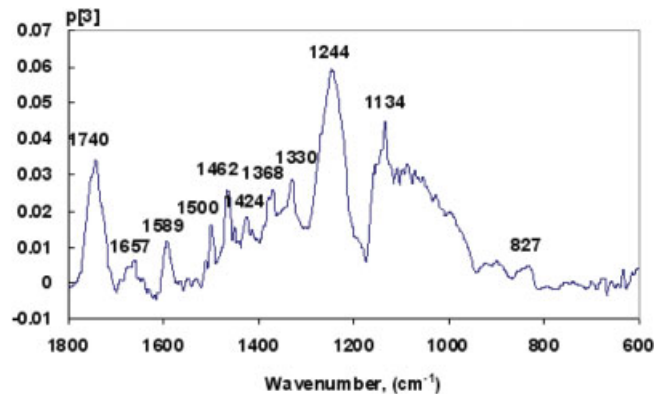
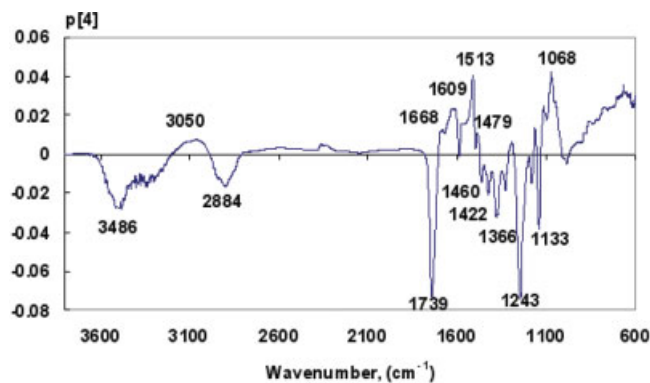


Figure 2 Loading line plot of the third principal component of the PCA model of the extracted hardwood samples. [Color figure can be viewed in the online issue, which is available at [www.interscience.wiley.com](http://www.interscience.wiley.com).]



**Figure 3** Loading line plot of the fourth principal component of the PCA model of the DRIFT spectral data collected from extracted hardwood samples. [Color figure can be viewed in the online issue, which is available at [www.interscience.wiley.com](http://www.interscience.wiley.com).]

positive scores in the direction of the fourth principal component (positive bands in Fig. 3) could have contained more tanninlike (or other unsaturated structures) than the samples with negative scores. The fourth loading line plot also exhibited a shoulder at  $1550\text{ cm}^{-1}$ , which could have resulted from oxidized lignin structures or, alternatively, from protein.<sup>33</sup>

Several bands typical of lignin were observed in the fifth loading plot (Fig. 4). In addition to the aromatic ring bands ( $1605$ ,  $1507$ , and  $1417\text{ cm}^{-1}$ ), the loading spectrum exhibited IR vibrations at  $1285$  and  $1271\text{ cm}^{-1}$ , which have previously been reported to be due to condensed<sup>36</sup> and noncondensed<sup>32</sup> guaiacyl (G) structures, respectively. Tannins could have possibly contributed to the shoulder at  $1700$ – $1620\text{ cm}^{-1}$ , and therefore, they could have also impacted the other aromatic absorptions. The aforementioned structures, which were condensed G, tannin, or both, were particularly enriched in samples 16, 20, and 24. The fin-

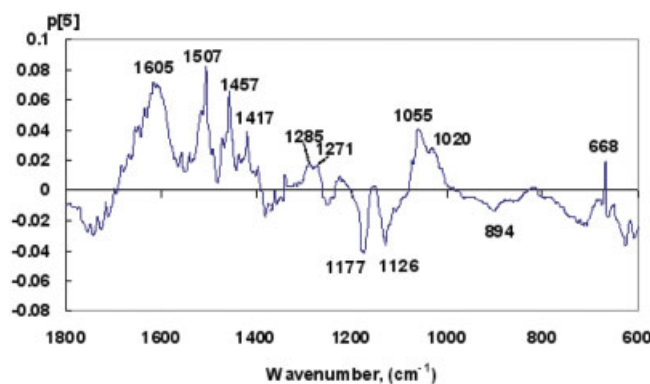


**Figure 4** Loading line plot of the fifth principal component of the PCA model of the DRIFT spectral data collected from extracted hardwood samples. [Color figure can be viewed in the online issue, which is available at [www.interscience.wiley.com](http://www.interscience.wiley.com).]

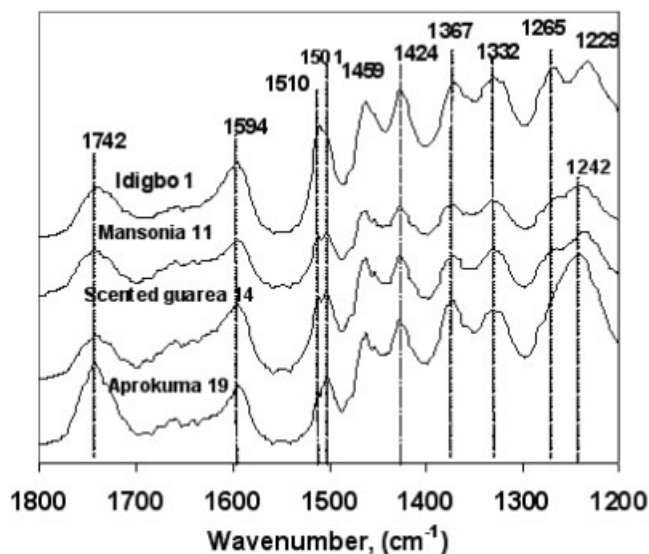


**Figure 5** DRIFT spectra of the four tropical hardwood samples. The numbers 1, 11, 14, and 19 alongside the spectra denote *T. ivorensis*, *M. altissima*, *G. cedrata*, and *A. micraster*, respectively.

gerprint bands at  $1055$ ,  $1020$ , and  $668\text{ cm}^{-1}$  most probably occurred due to the lignin or carbonyl structures; hence, the vibrations in the wave-number region  $1075$ – $1020$  were assigned to C—O stretching of alcohols, ethers, and carbonyl groups. The band at  $668\text{ cm}^{-1}$  could have been due to alkene C—H bending.<sup>33</sup>

FTIR spectra of the idigbo,<sup>1</sup> mansonia,<sup>11</sup> scented guarea,<sup>14</sup> and aprokuma<sup>19</sup> samples are presented in Figure 5. Each spectrum showed some distinctive features reflecting the differences in their lignin structure and carbohydrate composition. There was a small shift in the asymmetric aromatic ring absorbance maxima between the samples. Sample 19 had the maximum at  $1501\text{ cm}^{-1}$ , whereas that of sample 1 was located at  $1510\text{ cm}^{-1}$ . Samples 11 and 14 clearly exhibited two absorption bands at  $1510$  and  $1501\text{ cm}^{-1}$ . It is known that an increase in the amount of S units in lignin tends to shift the aromatic ring maximum toward lower wave numbers.<sup>32</sup> The band at  $1265\text{ cm}^{-1}$  typical of G lignin was seen most clearly in the spectrum of sample 1, whereas the other samples had only a shoulder around  $1265\text{ cm}^{-1}$ . This was not resolved at all in the spectrum of sample 19. These results indicate that samples 1 and 19 contained the highest amount of G and S units, respectively, whereas G and S unit contents for samples 11 and 14 were most probably intermediate.

The variation in the ratio of G and S units in lignin was also observed for other tropical wood samples. The band at  $1265\text{ cm}^{-1}$  was not discernable in all spectra due to the overlapping xylan band at  $1240\text{ cm}^{-1}$ , but differences in the maxima of the asymmetric aromatic ring band revealed that most of the durable

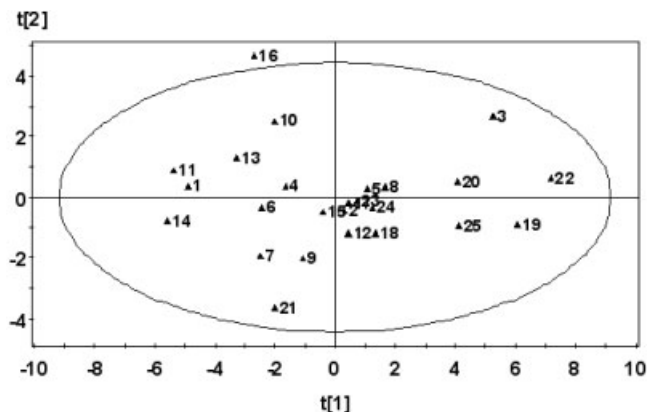


**Figure 6** Score scatter plot of the first and second principal components of the UVRR spectral data of the extracted hardwood samples.

and very durable samples (except samples 3 and 5) had maximums at longer wave numbers around  $1510\text{ cm}^{-1}$ , which indicated that their lignins may have contained more G than S units. However, some samples of low durability (two out of eight samples) had the aromatic band maximum around  $1510\text{ cm}^{-1}$ . According to the PCA analysis, samples 18 and 19 had a larger proportion of S units (Fig. 2), which was also in line with the position of the aromatic band maximum of the samples ( $1503\text{ cm}^{-1}$ ). It is possible that tannins or aromatic compounds contributed to the aromatic ring band and, thus, could also have had an impact on the band maximum shift. Consequently, no straightforward conclusions of the relationship between G type lignin content and bioresistance could be drawn on the basis of the FTIR results.

Of the spectra in Figure 5, sample 19 clearly had the strongest band at  $1740\text{ cm}^{-1}$  due to the  $\text{C}=\text{O}$  vibrations of acetyl groups in xylan. Furthermore, it also exhibited an intense band at  $1240\text{ cm}^{-1}$ , which was related to the  $\text{C}-\text{O}$  vibration of acetyl groups in xylan.<sup>30</sup> This was also shown by the PCA of the FTIR spectral data. It was obvious that sample 19 contained large amount of hemicelluloses, particularly, xylan. The  $\alpha$ -cellulose content for sample 19 was 47% (w/w), whereas that of acetyl bromide lignin was 19% (w/w), which was the lowest of all the samples.

### UVRR spectroscopy

The UVRR spectral data of the tropical hardwoods were subjected to PCA analysis. The scores of the first and second principal components are plotted in Figure 6. Positive and negative bands in the loading spectrum (Fig. 7) described enriched structures, especially in samples 1, 11, 13, and 14 and 3, 19, 20, 22, and 25, respectively. The bands at  $1601$  and  $1507\text{ cm}^{-1}$  were associated with the samples exhibiting positive

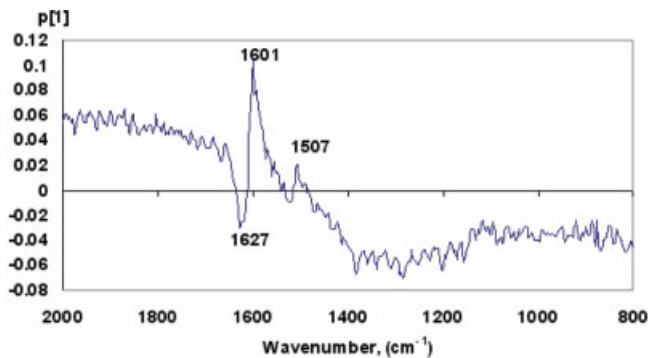


**Figure 7** Loading line plot of the first principal component of the PCA model of the UVRR spectral data collected from the 25 tropical hardwood samples. [Color figure can be viewed in the online issue, which is available at [www.interscience.wiley.com](http://www.interscience.wiley.com).]

score 1 loadings.<sup>3,19,20,22,25</sup> The signals at  $1601$  and  $1507\text{ cm}^{-1}$  were characteristic for the symmetric and asymmetric aromatic ring vibrations, respectively. Previously, the band at  $1507\text{ cm}^{-1}$  was identified in the UVRR spectrum of birch wood, and it was associated with S-type lignin structures.<sup>16</sup> The negative band at  $1627\text{ cm}^{-1}$ , as shown in Figure 7, has been observed in the UVRR spectrum of conjugated double-bond systems.<sup>19,20</sup> The spectral differences due to the second principal component (Fig. 8) arose from aromatic ring ( $1612\text{ cm}^{-1}$ ) and unsaturated structures ( $1567\text{ cm}^{-1}$ ). The samples shown in Figure 6 were not segregated in the same way as in the PCA of the FTIR spectral data, although samples 1 and 19 were among the two extremes in both PCA models.

A score scatter plot of the third and fourth principal components is presented in Figure 9. The positive bands at  $1638$  and  $1593\text{--}1530\text{ cm}^{-1}$  in the loading line plot of the third principal component (Fig. 10) suggest that samples 8, 18, and 24 shown in the score scatter plot (Fig. 9)

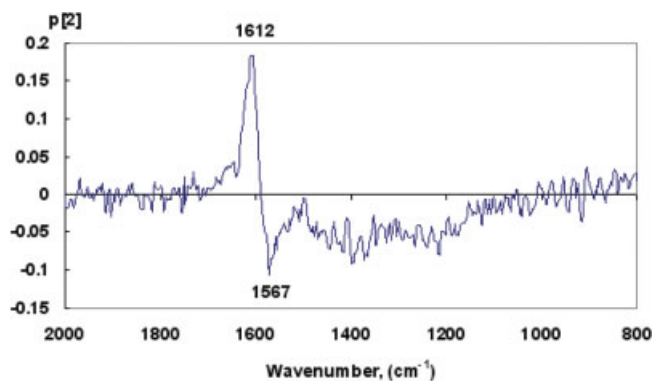


**Figure 8** Loading line plot of the second principal component of the PCA model of the UVRR spectral data collected from the 25 tropical hardwood samples. [Color figure can be viewed in the online issue, which is available at [www.interscience.wiley.com](http://www.interscience.wiley.com).]

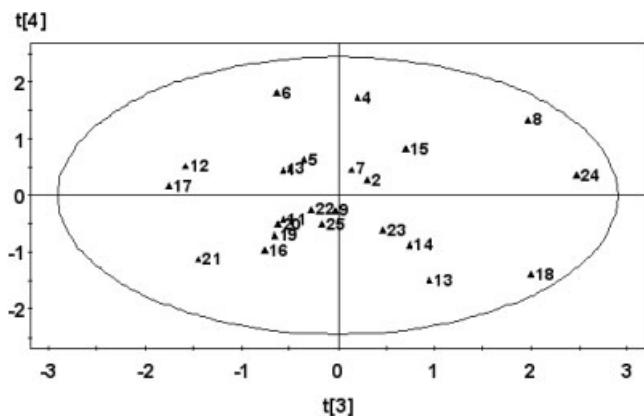


**Figure 9** Score scatter plot of the third and fourth principal components of the UVRR spectral data of the extracted hardwood samples.

contained more conjugated unsaturated structures.<sup>19,20</sup> According to the studies of Saariaho et al.,<sup>37</sup> the UVRR bands in the region of 1593–1530  $\text{cm}^{-1}$  were assigned to signals from C=C structures conjugated with aromatic ring and C<sub>5</sub> condensed structures. Increased amount of conjugated structures were detected in the region 1660–1620  $\text{cm}^{-1}$  in the FTIR spectra of these samples. In this IR region, absorptions mainly arise from conjugated carbonyl structures.<sup>33</sup> Furthermore, the loading spectrum of the FTIR data suggest that sample 24 contained condensed structures originating from lignin or condensed tannins. Negative bands in the UVRR loading plot (Fig. 10) at 1612, 1334, and 1285  $\text{cm}^{-1}$  suggest that samples 12, 17, and 21 were enriched in lignin structures. In addition to the aromatic ring signal at 1612  $\text{cm}^{-1}$ , the band at 1334  $\text{cm}^{-1}$  was assigned to S structures, whereas the signal at 1285  $\text{cm}^{-1}$  was characteristic for G structures.<sup>32</sup>

The loading line plot of the fourth principal component separated samples due to the conjugated structure or structures (Fig. 11). The positive bands at 1600

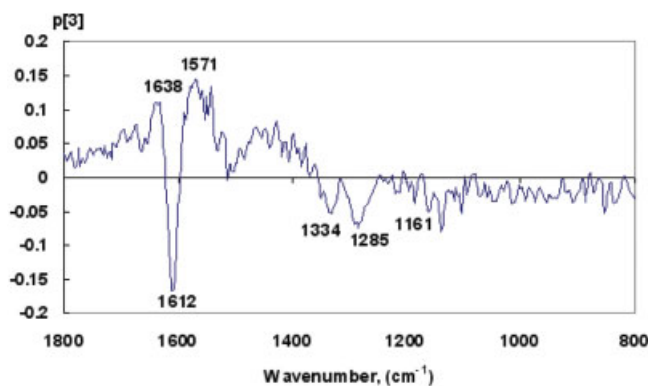


**Figure 10** Loading line plot of the third principal component of the PCA model of the UVRR spectral data collected from the 25 tropical hardwood samples. [Color figure can be viewed in the online issue, which is available at [www.interscience.wiley.com](http://www.interscience.wiley.com).]

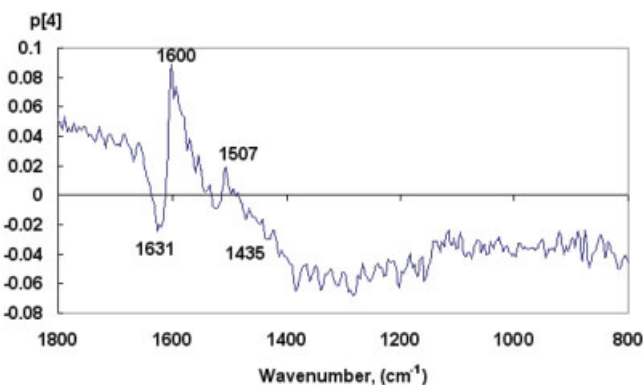


**Figure 11** Loading line plot of the fourth principal component of the PCA model of the UVRR spectral data collected from the 25 tropical hardwood samples. [Color figure can be viewed in the online issue, which is available at [www.interscience.wiley.com](http://www.interscience.wiley.com).]

and 1507  $\text{cm}^{-1}$  associated particularly with samples 6, 4, and 8 originated from symmetric and asymmetric aromatic ring vibrations, respectively.<sup>20</sup> Only one negative band at 1631  $\text{cm}^{-1}$ , due to conjugated double bonds, was clearly observable in Figure 11. It was not possible to resolve the Raman signals in the region 1480–1140  $\text{cm}^{-1}$  (Fig. 11) due to baseline variation and spectral noise.

### <sup>13</sup>C-NMR CP-MAS spectroscopy

Solid state <sup>13</sup>C-NMR CP-MAS analyses were undertaken alongside the FTIR and UVRR measurements to give additional and complementary information on the chemical structure of several tropical hardwoods. Only the NMR CP-MAS spectra of the idigbo,<sup>1</sup> mansonia,<sup>11</sup> scented guarea,<sup>14</sup> and aprokuma<sup>19</sup> samples are presented as they offer quite an extensive overview of all of the wood samples in relation to both the chemical structure and bioresistance. All of these wood species were from different tree families associated with different chemical structures. The bioresistances of samples 1, 11, 14, and 19 were classified as durable, very durable, durable–moderate, and low, respectively, as is shown in Table I.

Cellulose, hemicelluloses, and lignin gave characteristic signals in the solid-state NMR spectrum shown in Figure 12. Sharp signals were assigned to cellulose and hemicelluloses. The signals at 72–75 ppm were assigned to the C-2, C-3, and C-5 carbons of cellulose, and the signal at 105 ppm was assigned to the cellulose C-1. Distinct signals for amorphous and crystalline carbons could be detected. The signals at 89 and 65 ppm were assigned to the more ordered cellulose C-4 and C-6 carbons, respectively, whereas the signals at 84 and 62 ppm were assigned to the less ordered cellulose C-4 and C-6 carbons.<sup>38–40</sup>

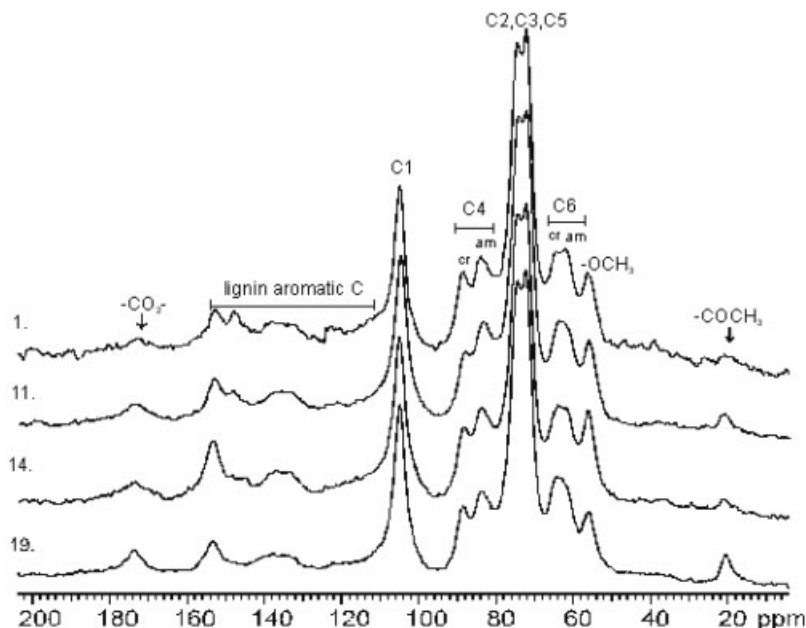


**Figure 12**  $^{13}\text{C}$ -NMR CP-MAS spectra of the four tropical hardwood samples. The numbers 1, 11, 14, and 19 alongside the spectra denote *T. ivorensis*, *M. altissima*, *G. cedrata*, and *A. micraster*, respectively.

CP-MAS spectra revealed differences in chemical structure and composition between the samples. The signals in the spectra were divided into eight groups, the assignments and chemical shifts of which are given in Table III. The percentage values of carbons were calculated from the integrated intensities of signals within each shift range to make a comparison between the chemical structures of the samples. Total carbon signal intensity was 100, and the relative signal intensities in the CP-MAS spectra are shown graphically in Figure 13. Although the solid-state NMR spectrum was not quantitative, the relative intensities of the signals between the spectra measured under identical conditions could be compared at least internally.

In the carbohydrate area, there were differences between the samples, especially in the cellulose C-4 region shown in Figures 12 and 13. The relative inten-

sities of the crystalline (at 89 ppm) and amorphous (at 84 ppm) cellulose signals varied between the wood samples, which indicated a varying cellulose crystalline structure in different wood species. The amount of crystalline cellulose appeared to be the smallest in sample 11, according to the ratio of the crystalline and amorphous cellulose C-4 signals. However, conventional CP-MAS spectra of wood contained several signal overlaps. The signals of cellulose were overlapped by the signals of hemicelluloses and lignin, and hence, the CP-MAS spectra might have given inaccurate information on cellulose crystallinity.<sup>41-43</sup>

The investigation of the hemicelluloses in CP-MAS spectra was complicated due to the strong overlap of the signals assigned to cellulose and lignin. Only the

**TABLE III**  
Chemical-Shift Ranges of Different Types of Carbon Atoms in  $^{13}\text{C}$ -NMR CP-MAS Spectra

NMR spectral region	Shift range (ppm)	Types of carbons
1	180–168	$\text{CO}_2$ in hemicelluloses
2	158–110	Aromatic C
3	109.8–100	C-1 of cellulose
4	92–80.5	C-4 of cellulose
5	80–68.5	C-2, C-3, and C-5 of cellulose
6	68–60	C-6 of cellulose
7	59–52	$\text{OCH}_3$
8	24–18	$\text{CH}_3$ in hemicelluloses

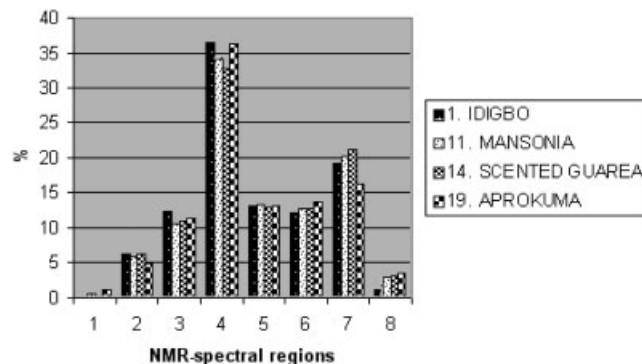


**Figure 13** Relative  $^{13}\text{C}$ -NMR CP-MAS signal intensities (total carbon signal intensity = 100) within the spectral regions defined in Table III of the four tropical hardwood samples.



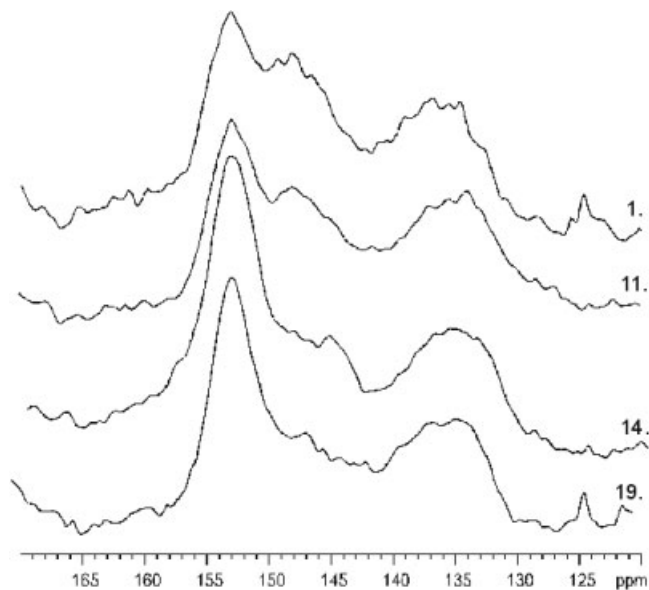


**Figure 14** DD NMR spectra of the four tropical hardwood samples. The numbers 1, 11, 14, and 19 alongside the spectra denote *T. ivorensis*, *M. altissima*, *G. cedrata*, and *A. micraster*, respectively.

signals of methyl (21 ppm) and carboxylic carbons (173 ppm) derived from acetyl groups attached to hemicelluloses were clear, although weak, in the CP-MAS spectra of wood. The relative intensities of these signals, as shown in Figure 12, differed between the wood species and was lowest for sample 1 and highest for sample 19, which suggested the highest amount of hemicelluloses in sample 19, which was also noticed in the FTIR spectra, as shown in Figure 5.

The broader signals in the NMR spectra (Fig. 12) between 110 and 155 ppm were assigned to various carbons in the lignin structure.<sup>27,44,45</sup> In addition, the signal at 56 ppm was assigned to methoxyl carbons in lignin. The amount of methoxyl groups was highest in sample 14 and smallest in sample 19 (Fig. 13). Furthermore, the amount of lignin relative to carbohydrates appeared to be lowest in sample 19 (Fig. 13), and this was contributed by the acetyl bromide lignin contents, which showed sample 19 to have the lowest level.

The lignin aromatic carbons could be studied more precisely by the DD technique. The DD spectra, as shown in Figure 14, showed a signal at 153 ppm assigned to the C-3 and C-5 carbons of S and C-4 of G units that were etherified at C-4. A signal at 148 ppm was assigned to the C-3 and C-5 carbons in nonetherified S units and the C-3 carbons of G units. The shoulder at 146 ppm was assigned to the C-4 carbons of G units that were nonetherified. The signal at 153 ppm was, thus, mainly from the S units that had  $\beta$ -O-4 linkages, and the signal at 148 ppm was mainly assigned to G units.<sup>26,43</sup> The signal at 136 ppm was assigned to the C-1 and C-4 carbons of S and the C-1

carbon of G units that were etherified, whereas the corresponding nonetherified structures gave a shoulder at 133 ppm.

In the DD spectra (Fig. 14), large differences in the ratio of the signals at 153 and 148 ppm were observed between the samples. As the amount of G units increased relative to the S units, the signal at 148 ppm became larger in relation to the signal at 153 ppm. The amount of G units was highest for sample 1 and diminished through samples 11 and 14 to sample 19, where it was smallest and reflected a predominant S-type lignin. The analogous results were reflected in the FTIR spectral data (Fig. 5). Higher amount of G units correlated with a higher amount of lignin, according to Table II. In addition, higher amounts of G units and lignin appeared to correlate with better bioresistance. The FTIR spectra indicated that majority of the durable species except few samples (samples 3 and 5) contained more G than S units, but also some samples of low durability consisted mainly of G lignin (samples 6 and 24). The signal at 145 ppm, which was very clear, especially in the DD spectrum of sample 14, as shown in Figure 14, was due to condensed tannins.<sup>46–47</sup> The signal of tannins was weaker and not well resolved in the other spectra due to overlapping lignin signals. The FTIR data also indicated that sample 14 might have contained tannin-related substances due to the rather strong absorptions in the spectral region of 1660–1620  $\text{cm}^{-1}$ .

## DISCUSSION

All of the methods provided unique information on the tropical hardwood samples. PCA of the UVRR spectral data segregated samples according to various aromatic and other unsaturated structures, whereas the most prominent principal components of the FTIR data gave separation of the samples according to the variation of hemicellulose and lignin contents and structures and the amount and type of the carbonyl structures. Furthermore, NMR data showed dissimilarities in the amount of crystalline cellulose and hemicelluloses.

The density data, content of lignin, and acetone-soluble substances of the tropical woods are shown in Table II. Biological durability classes for the most of the studied wood species were found from Web sites.<sup>48,49</sup> In most cases, durable and very durable species had a high lignin content and/or high density. The FTIR data revealed that a higher content of G units correlated in many cases with a higher amount of acetyl bromide lignin. NMR data from four representative samples were in line with this observation. Moreover, a higher amount of G units appeared to be related to better bioresistance, according to the NMR and FTIR data, although there were samples of low durability that had more G-type than S-type units as well. Thus, the type and amount of lignin were not the

only factors confirming biological resistance. Analysis of the acetone-soluble compounds varied to a large extent within the samples (0.5–6.6% w/w) and also between durable wood species. The amount of acetone-soluble substances for durable samples 1, 3, 5, and 11 was highest over 4% (w/w), whereas that for the other durable samples was in the range 0.6–3.6% (w/w; Table II). Consequently, there was no clear relationship between the amount of the acetone-extractable compounds and bioresistance of the samples, although the better biodurability of some samples was probably due to higher amounts of extractable substances. Previous studies have also shown that the bioresistance of some tropical wood species is related to the particular extractable toxic compounds.<sup>3</sup>

UVR spectroscopy data of the acetone-extracted wood samples indicated that some of the durable and very durable wood species were more abundant in aromatic or other unsaturated structures than the samples exhibiting lower biological durability. This suggests that unsaturated structures, at least partially, contribute to the fungal resistance of tropical woods. The bioresistance of tropical woods has been suggested to correlate with higher amounts of condensed G structures.<sup>12</sup> There were, however, no clear signs of condensation in the NMR spectra, not even in the spectra of samples 1 and 11, which contained relatively greater amounts of G units, although they reportedly exhibited a greater level of bioresistance than samples 19 and 14. In the NMR spectra, condensed structures gave a shoulder at 128 ppm.<sup>43</sup> PCA of the FTIR and UVR spectroscopy data indicated that some of the extracted samples may have contained condensed aromatic structures of lignin or tannin origin, but the possible existences of these structures were not correlated with the biological durability of the samples.

It is obvious that biological durability of tropical woods is dependent on several factors, including density, lignin structure, content, and the amount and nature of extractable compounds, and thus, no straightforward relationships between durability and a particular chemical or other factor could be made.

The authors thank and acknowledge Barry Gardiner from Forest Research for the tropical hardwood samples and Rita Hatakka for collecting the UVR spectra.

## References

- Williams, R. S.; Miller, R.; Gangstad, J. *Wood Fiber Sci* 2001, 33, 618.
- Huang, Z.; Maher, K.; Amarty, S. Presented at the International Research Group on Wood Preservation, 35th Annual Meeting, Ljubljana, Slovenia, June 2004.
- Onuorah, E. O. *Bioresour Technol* 2000, 75, 171.
- Kishino, M.; Nakano, T. *Holzforchung* 2004, 58, 552.
- Kishino, M.; Nakano, T. *Holzforchung* 2004, 58, 558.
- Eslyn, W. E.; Bultman, J. D.; Jurd, L. *Physiol Biochem* 1981, 71, 521.
- Yap, M. G. S. *J. Wood Chem Technol* 1987, 7, 343.
- Fengel, D.; Greune, A.; Wegener, G. *Holzforchung* 1983, 37, 121.
- Pastore, T. C. M.; Santos, K. O.; Rubim, J. C. *Bioresour Technol* 2004, 93, 37.
- Saka, S. In *Wood and Cellulosic Chemistry*, 2nd ed.; Hon, D. N.-S.; Shiraishi, N., Eds.; Marcel Dekker: New York, 2001; pp 51.
- Owen, N. L.; Thomas, D. W. *Appl Spectrosc* 1989, 43, 451.
- Martínez, A. T.; Almendros, G.; González-Vila, F. J.; Fründ, R. *Solid State Nucl Magn Reson* 1999, 15, 41.
- Martínez, A. T.; González, A. E.; Prieto, A.; González-Vila, F. J.; Fründ, R. *Holzforchung* 1991, 45, 279.
- Sosanwo, O. A.; Fawcett, A. H.; Apperley, D. *Polym Int* 1995, 36, 247.
- Nogueira, M. C. J. A.; Tavares, M. I. B.; Nogueira, J. S. *Polymer* 2004, 45, 1217.
- Saariaho, A.-M.; Jääskeläinen, A.-S.; Nuopponen, M.; Vuorinen, T. *Appl Spectrosc* 2003, 57, 58.
- Nuopponen, M.; Vuorinen, T.; Jämsä, S.; Viitaniemi, P. *J. Wood Chem Technol* 2004, 24, 13.
- Saariaho, A.-M.; Hortling, B.; Jääskeläinen, A.-S.; Tamminen, T.; Vuorinen, T. *J. Pulp Pap Sci* 2003, 29, 363.
- Nuopponen, M.; Willför, S.; Jääskeläinen, A.-S.; Sundberg, A.; Vuorinen, T. *Spectrochim Acta Part A* 2004, 60, 2953.
- Nuopponen, M.; Willför, S.; Jääskeläinen, A.-S.; Vuorinen, T. *Spectrochim Acta Part A* 2004, 60, 2963.
- Brendel, O.; Iannetta, P. P. M.; Stewart, D. A. *Phytochem Anal* 2000, 11, 7.
- Johnson, D. B.; Moore, W. E.; Zank, L. C. *Tappi* 1961, 44, 793.
- Iiyama, K.; Wallis, A. F. A. *Wood Sci Technol* 1988, 22, 271.
- Horii, F.; Hirai, A.; Kitamaru, R.; Sakurada, I. *Cellul Chem Technol* 1985, 19, 513.
- Willis, J. M.; Herring, F. G. *Macromolecules* 1987, 20, 1554.
- Hatcher, P. G. *Org Geochem* 1987, 11, 31.
- Haw, J. F.; Maciel, G. E.; Schroeder, H. A. *Anal Chem* 1984, 56, 1323.
- Manders, W. F. *Solid-State Holzforchung* 1987, 41, 13.
- Gerasimowicz, W. V.; Hicks, K. B.; Pfeffer, P. E. *Macromolecules* 1984, 17, 2597.
- Harrington, K. J.; Higgins, H. G.; Michell, A. J. *Holzforchung* 1964, 18, 108.
- Kačuráková, M.; Wellner, N.; Ebringerová, A.; Hromádková, Z.; Wilson, R. H. *Food Hydrocolloids* 1999, 13, 35.
- Faix, O. *Holzforchung* 1991, 45 (Suppl.), 21.
- Williams, D. H.; Fleming, I. In *Spectroscopic Methods in Organic Chemistry*, 5th ed.; McGraw-Hill: Maidenhead, England, 1995; p 28.
- Peng, S.; Scalbert, A.; Monties, B. *Phytochemistry* 1991, 30, 775.
- Lange, W.; Faix, O. *Holzforchung* 1991, 53, 519.
- Åkerholm, M.; Salmén, L. *Holzforchung* 2003, 57, 459.
- Saariaho, A.-M.; Argyropoulos, D. S.; Jääskeläinen, A. S.; Vuorinen, T. *Vib Spectrosc* 2005, 37, 111.
- Atalla, R. H.; VanderHart, D. L. *Solid State Nucl Magn Reson* 1999, 15, 1.
- Earl, W. L.; VanderHart, D. L. *Macromolecules* 1981, 14, 570.
- VanderHart, D. L.; Atalla, R. H. *Macromolecules* 1984, 17, 1465.
- Sivonen, H.; Maunu, S. L.; Sundholm, F.; Jämsä, S.; Viitaniemi, P. *Holzforchung* 2002, 56, 648.
- Andersson, S.; Wikberg, H.; Pesonen, E.; Maunu, S. L.; Serimaa, R. *Trees* 2004, 18, 346.
- Wikberg, H.; Maunu, S. L. *Carbohydr Polym* 2004, 58, 461.
- Leary, G. J.; Morgan, K. R.; Newman, R. H.; Samuelsson, B.; Westermarck, U. *Holzforchung* 1986, 40, 221.
- Haw, J. F.; Maciel, G. E.; Biermann, C. J. *Holzforchung* 1984, 38, 327.
- Leary, G. J.; Newman, R. H.; Morgan, K. R. *Holzforchung* 1986, 40, 267.
- Morgan, K. R.; Newman, R. H. *Appita* 1987, 40, 450.
- Wood Properties/Tropical Hardwood, <http://www2.fpl.fs.fed.us/TechSheets/tropicalwood.html>, accessed February 2005.
- South American Woods, <http://www.cirad.fr/activites/bois/en/syst/america/cedro.pdf>, accessed February 2005.